Changes in Orientation of Actin during Contraction of Muscle

J. Borejdo,* A. Shepard,* D. Dumka,* I. Akopova,* J. Talent,* A. Malka,* and T. P. Burghardt†
*Department of Molecular Biology and Immunology, University of North Texas, Fort Worth, Texas and
†Department of Biochemistry and Molecular Biology, Mayo Foundation, Rochester, Minnesota

ABSTRACT It is well documented that muscle contraction results from cyclic rotations of actin-bound myosin cross-bridges. The role of actin is hypothesized to be limited to accelerating phosphate release from myosin and to serving as a rigid substrate for cross-bridge rotations. To test this hypothesis, we have measured actin rotations during contraction of a skeletal muscle. Actin filaments of rabbit psoas fiber were labeled with rhodamine-phalloidin. Muscle contraction was induced by a pulse of ATP photogenerated from caged precursor. ATP induced a single turnover of cross-bridges. The rotations were measured by anisotropy of fluorescence originating from a small volume defined by a narrow aperture of a confocal microscope. The anisotropy of phalloidin-actin changed rapidly at first and was followed by a slow relaxation to a steady-state value. The kinetics of orientation changes of actin and myosin were the same. Extracting myosin abolished anisotropy changes. To test whether the rotation of actin was imposed by cross-bridges or whether it reflected hydrolytic activity of actin itself, we labeled actin with fluorescent ADP. The time-course of anisotropy change of fluorescent nucleotide was similar to that of phalloidin-actin. These results suggest that orientation changes of actin are caused by dissociation and rebinding of myosin cross-bridges, and that during contraction, nucleotide does not dissociate from actin.

INTRODUCTION

Rotational motions associated with muscle contraction may occur in myosin, actin, or in both (Huxley and Simmons, 1971). Rotations of myosin cross-bridges are well documented (Dos Remedios et al., 1972; Nihei et al., 1974; Thomas and Cooke, 1980; Borejdo et al., 1982, 2002b; Sabido-David et al., 1998; Allen et al., 1996; Hopkins et al., 1998; Borejdo and Akopova, 2003), but changes in actin have not been thoroughly investigated. F-actin (Oosawa et al., 1977; Oosawa, 1977) and G-actin (Page et al., 1998; Galkin et al., 2002) are dynamic structures displaying many internal degrees of freedom, so it is likely that the interactions with myosin have an affect on conformation. Indeed, dissociation of myosin heads from actin results in a change of fluorescence polarization (Borovikov and Chernogriadskaia, 1979; Borovikov et al., 1982; Prochniewicz-Nakayama et al., 1983) and in change of μs-rotational motion detected by saturation transfer electron paramagnetic resonance spectra of spin labels on Cys-374 of actin (Thomas et al., 1979). However, active interaction of heads with actin were found not to induce μs-rotational motions of Cys-374 (Ostap and Thomas, 1991).

In this article we studied kinetics of orientation changes of actin during the power-stroke of skeletal muscle. A narrow aperture of a confocal microscope defined a small volume within a thin filament. Rotational motion of a small number of actin monomers within this volume was synchronized by rapidly stimulating muscle by a short pulse of ATP. The amount of photogenerated ATP was enough for a single turnover of nucleotide by the cross-bridges. The anisotropy of phalloidin bound to actin changed rapidly at first and was followed by a slow relaxation back to a steady-state value, which was different from the original anisotropy. The rates of orientation change of actin monomers broadly paralleled rates of rotations of myosin heads observed earlier (Borejdo and Akopova, 2003).

The observed rotations of actin could be induced passively—i.e., be imposed by myosin heads, or actively—i.e., reflect hydrolytic activity of actin itself. Active involvement of actin is consistent with the fact that actin polymerization-depolymerization may play a role in contraction of smooth muscle (Barany et al., 2001). The interest in the active involvement of actin has recently been reactivated by the demonstration that in vitro interactions of the myosin motor domain with actin change the actomyosin interface to produce hot-spots of activity (Tanaka et al., 2002; Nishikawa et al., 2002). These spots propagate along actin filaments to enable myosin V or VI to produce large processive steps during translocation along actin. The active role of actin requires that it hydrolyzes ATP, i.e., that during contraction actin-bound ADP is released from the enzyme and is replaced with excess ATP from the solvent. To test whether such nucleotide exchange occurs during contraction, we have incorporated a fluorescent analog of ATP (Alexa-ATP) into actin and followed its rotation after photogenerating excess nonfluorescent ATP in the solvent. If the nucleotide were hydrolyzed and Alexa-ADP released into a solvent, the anisotropy of fluorescent moiety would not change, because actin-bound Alexa-ADP has similar anisotropy as free Alexa-ADP (because of the short fluorescence lifetime of Alexa-ATP). Instead, anisotropy changes of fluorescent nucleotide were identical to the changes of phalloidin-actin. This suggests that ADP is not released from actin during muscle

Submitted June 19, 2003, and accepted for publication December 1, 2003.

Address reprint requests to Julian Borejdo, University of North Texas, Dept. of Biochemistry, Health Science Center, 3500 Camp Bowie Blvd., Fort Worth, TX 76107-2699. Tel.: 817-735-2699; E-mail: jborejdo@hsc.unt.edu.

0006-3495/04/04/2308/10 $2.00

contraction, consistent with earlier work which showed that <20% of bound nucleotide was released during superprecipitation of skeletal actomyosin (Strzelecka-Golaszewska et al., 1975). We suggest that actin rotations are passive, i.e., that rotations of myosin cross-bridges induce parallel motions of actin monomers in a thin filament.

MATERIALS AND METHODS

Chemicals and solutions

Standard chemicals, nucleotides, and phalloidin coupled to fluorescein-5(6)-isothiocyanate (FITC-phalloidin) were from Sigma (St. Louis, MO). 5′-iodoacetamido-tetramethyl-rhodamine-phalloidin (Rh-phalloidin), 5-dimethyoxy-2-nitrobenzyl-caged ATP (DMNPE-caged ATP), Alexa647-ATP, and 1-(4,5-dimethoxy-2-nitrophenyl)-1,2- diaminoethane-*n*,*n*, *n*′,*n*′-tetra-acetic acid (DMNP-EDTA) were from Molecular Probes (Eugene, OR). Cy5-ATP was a gift from Dr. D. Root (University of North Texas). The composition of solutions is given in Table 1. All solutions used in the photolysis experiments contained 10 mM of reduced glutathione. The glycerinating solution contained 80 mM K-acetate, 0.2 mg/mL PMSF, 2 mM mercaptoethanol, and 50% glycerol.

Labeling of actin in muscle fibers with phalloidin

Muscle fibers were glycerinated and isolated as described earlier (Borejdo et al., 2002b). The fibers in the relaxing solution were labeled with 0.3 μM Rh- or FITC-phalloidin for 15 min at room temperature. After labeling, the fibers were thoroughly washed with the relaxing solution and, when necessary, by a Ca^{2+}-rigor solution. Tension development was studied by MKB force transducer (Scientific Instruments, Heidelberg, Germany). Control (unlabeled) fibers developed 0.96 ± 0.05 mN/fiber of maximum isometric tension ($n = 32$, mean ± SE). Fibers labeled with 0.3 μM Rh-phalloidin developed tension within 10% of control. The lack of effect on tension is in agreement with earlier results (Bukatina et al., 1996). The degree of labeling was estimated by comparing fluorescent intensity of fiber with the intensity of known concentrations of Rh-phalloidin. Fig. 1 *A* shows the dependence of the fluorescent intensity of a fiber (viewed with a wide-field microscope using a 10×, $NA = 0.22$ objective) on the concentration of Rh-phalloidin in labeling solution. Fig. 1 *B* shows the fluorescent intensity of different concentrations of solutions of Rh-phalloidin. The intensity of fluorescence of Rh-phalloidin increased in the presence of F-actin 3.1 times at 1 μM dye, and 1.4 times at 5 μM dye. Smaller increase is no doubt due to the insufficient excess of actin (it was impossible to do experiments using larger excess because of viscosity of F-actin). By comparing Fig. 1, *A* and *B*, we estimate that after 15 min of incubation with 0.3 μM phalloidin, the concentration of fluorescent phalloidin in muscle was ~4–5 μM. Number of actin molecules observed by the confocal microscope is equal to this concentration multiplied by the experimental volume. The confocal volume was ~0.3 μm^3. There are ~1000 labeled actin monomers in this volume.

TABLE 1 Composition of solutions

Solution	$MgCl_2$	$CaCl_2$	EGTA	EDTA	ATP	KCl
G-buffer		0.1			0.2	
EGTA-rigor	4		2			50
EDTA-rigor				2		50
Ca^{2+}-rigor	4	0.1				50
Relaxing	4		2		5	50
Glycerinating	2		5		5	50

All solutions contained 10 mM Tris-HCl buffer, pH 7.5. Ca^{2+}-rigor solution contained 10 mM glutathione. Concentrations in mM.

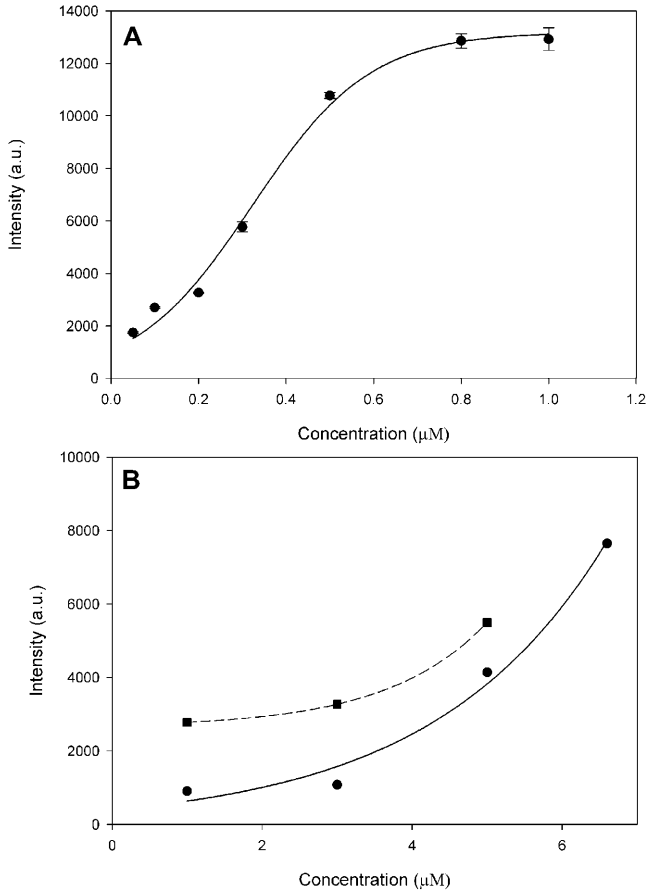

FIGURE 1 Binding of Rh-phalloidin to a muscle fiber. (*A*) Single muscle fiber was irrigated with varying concentrations of Rh-phalloidin for 15 min at room temperature. The fluorescence intensity was recorded through 10× ($NA = 0.22$) objective of the wide-field microscope after washing out the excess of phalloidin. Bars, mean ± SD of three experiments. (*B*) Fluorescence intensity of known concentrations of Rh-phalloidin viewed through the same microscope optics. (*Solid line*) Rh-phalloidin in Ca-rigor, and (*dashed line*) Rh-phalloidin + 5 μM actin in Ca-rigor. $\lambda_{ex} = 543$ nm.

Specificity of labeling

The specificity of labeling was assessed by inspecting the striation pattern. To maximize the resolution and reduce thickness of the section, the diameter of the confocal pinhole was minimized (to 26.3 μm, 0.65 μm on image plane). Fig. 2 *A* shows the confocal image of FITC-phalloidin-labeled fiber. The striation pattern is impossible to visualize without a confocal aperture (Fig. 2 *B*). The white spot (indicated by an *arrowhead*) shows the relative size of the probing laser beam. The observed volume is shown schematically in Fig. 2 *C*. Its width and depth are approximately equal to the diffraction limit (~0.3 μm) of the illuminating laser spot. Its height is limited by the confocal aperture (1.35 Airy units) to ~3 μm, giving the volume of 0.3 μm^3. The average intensity of the dark (myosin) bands was ~150 times smaller than the intensity of light (actin) bands. In agreement with earlier observations on isolated myofibrils (Szczesna and Lehrer, 1993; Ao and Lehrer, 1995; Zhukarev et al., 1997) phalloidin was not distributed uniformly along the length of a thin filament. This nonuniformity was independent of labeling times, the stretch, or the type of dye coupled to phalloidin. The specificity was further assessed by co-labeling actin and myosin. Myosin was first labeled by exchanging its native essential light chain-3 with fluorescent light chain-3 that had been prelabeled with 5′-

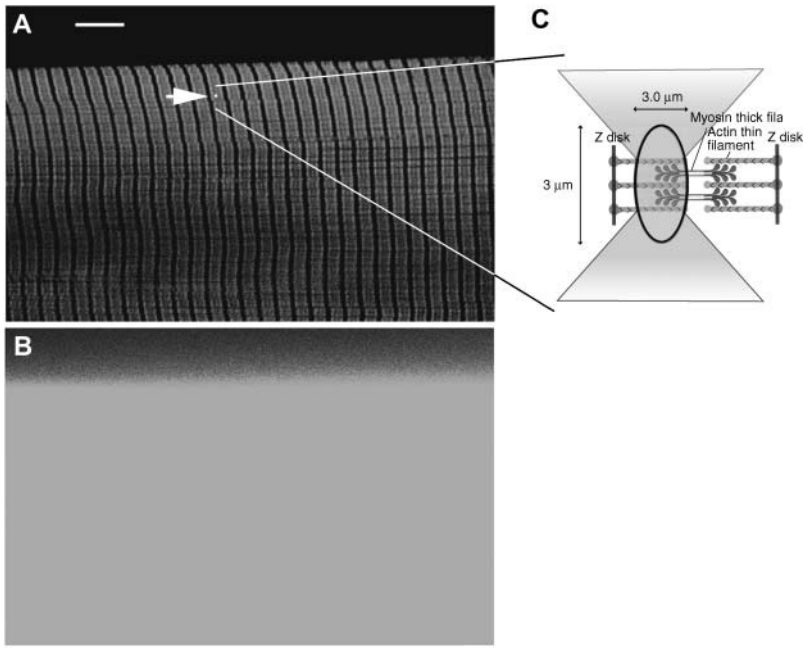

FIGURE 2 Labeling thin filaments in a fiber. (*A*) Fiber labeled with FITC-phalloidin viewed through confocal aperture. Fluorescein filter (band-pass $515 < \lambda < 565$ nm). The arrowhead points to a spot that indicates the position of the laser beam. Bar = 10 μm, sarcomere length = 2.8 μm. (*B*) The same fiber viewed without confocal aperture. (*C*) Schematic illustration of the experimental volume. Laser beam is focused to a diffraction limit. The light is collected from a volume defined by ellipsoid of revolution with diameters 0.3 and 3 μm. There are ~1000 fluorescent actin monomers in this volume.

iodoacetamido-tetramethyl-rhodamine (5′-IATR) (at Cys-178). Fibers were then labeled with FITC-phalloidin. Fig. 3 shows the appearance of the fiber through fluorescein (Fig. 3 *A*) and rhodamine (Fig. 3 *B*) filters to show the distribution of actin and myosin. The two images are combined in Fig. 3 *C* to show that, as expected, green FITC-phalloidin fluorescence and red Rh-phalloidin fluorescence originate from the I- and A-bands, respectively. There is some co-labeling in the overlap zone (indicated by *yellow patches*), but since actin is labeled to much greater extent than myosin, patches are not well resolved.

Labeling of actin in muscle fibers with fluorescent ATP

G-actin was prepared according to standard procedure (Spudich and Watt, 1971). 3.4 mg/mL G-actin was passed through a small Sephadex-50 column and incubated for 2 h in ice with G-buffer (Table 1) containing 50-μM fluorescent ATP instead of normal ATP. After incubation G-actin was passed again through a column to remove the excess of fluorescent ATP. The degree of labeling was ~45%. Fluorescent actin was used immediately after preparation. Thin filaments were extracted from muscle fiber and replaced with actin containing fluorescent ATP by a modification of the procedure (Fujita and Ishiwata, 1998). Briefly: 2 mg/mL gelsolin stock solution in G-buffer buffer was diluted just before the experiment to 0.3 mg/mL with G-buffer + 50 mM KCl. Thin filaments were removed by incubation for 80 min at 0°C. Fibers were then washed with cold EGTA-rigor. Just before experiment 20 μL G-actin was diluted to a final concentration of 1 mg/mL with EGTA-rigor solution containing 0.2 mM ATP and added to a fiber for 7 min in cold. The incubation-wash cycles were repeated three times. Finally, the fibers were washed with cold Ca-rigor solution. Tension developed by fibers labeled with Alexa-ATP was not measured. Labeling gave excellent striation patterns. Fibers labeled with Cy5-ATP showed weaker striations then fibers labeled with Alexa647-ATP.

Experimental arrangement

The instrument to measure anisotropy of fluorescence was described elsewhere (Borejdo et al., 2002b; Borejdo and Akopova, 2003). The current setup differs from the earlier one in that the laser spot is not scanned and that the 633-nm excitation and Cy5 emission filters have been added to detect fluorescent ATP. Briefly, muscle fiber is placed on a stage of a confocal microscope (Zeiss, LSM 410, Thornwood, NY). A 633-nm visible light from He/Ne laser is selected by the line selection filter to excite the fluorescent nucleotide on actin. Ar/Kr laser is selected by another line selection filter to excite FITC-phalloidin (488 nm) or Rh-phalloidin (568 nm). The polarization of the laser beam can be rotated by a $\lambda/2$ plate. It is directed by the dichroic mirror onto an objective (Zeiss C-Apo, 40×, NA

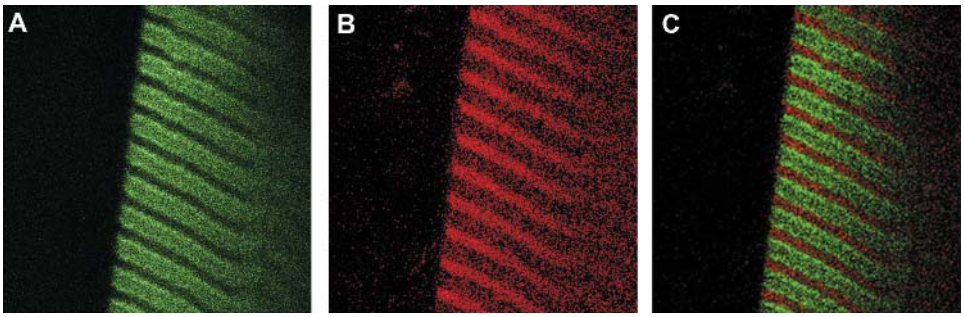

FIGURE 3 Actin labeled with FITC-phalloidin (*green*) and myosin labeled with essential light chain coupled to IATR (*red*) in the same muscle fiber. (*A*) Muscle viewed through fluorescein filter (band-pass $515 < \lambda < 565$ nm). Only the I-bands, containing fluorescent actin, are visible. (*B*) The same fiber viewed through rhodamine filter (long-pass $\lambda > 590$ nm). Only the A-bands, containing fluorescent myosin, are visible. (*C*) Composite of *A* and *B*. Sarcomere length = 2.65 μm.

1.2, water immersion). The ultraviolet (UV) beam of an argon laser operating at 364 and 351 nm is used to photolyze caged-nucleotide. The UV light is admitted by the shutter. Dichroic combiners merge the UV and visible beams. Objective focuses the exciting light on muscle, collects it, and projects fluorescent light onto the photomultipliers through orthogonally polarized analyzers.

Photogeneration of ATP

Muscle is perfused with 2 mM of 5-dimethyoxy-2-nitrobenzyl-caged ATP (DMNPE-caged ATP). The UV beam is focused by the objective to a Gaussian spot with width and length equal to twice the lateral resolution of the UV beam (~0.2 μm). The height equals to the depth-of-focus of the objective (~3.5 μm, confocal aperture does not decrease the depth-of-focus of excitation). A few seconds after the beginning of the experiment, the shutter admitting the UV light is opened for exactly 10 ms. The laser power incident on the illuminated area (0.04 μm^2) is 0.12 mJ/s. The energy flux through the illuminated area is 0.12 mJ/(s $\times$ 0.04 μm^2) = 3.0 mJ/(s $\times$ μm^2). ATP stays in the experimental volume on the average for 300 μs. The energy through the illuminated area during this time is 9×10^{-4} mJ/μm^2. This is larger than the energy flux obtainable with the frequency-doubled ruby laser ($\sim 3 \times 10^{-5}$mJ/μm^2) (Goldman et al., 1984). The amount of released ATP is enough for a single turnover of ATP by cross-bridges (Borejdo et al., 2002a; Borejdo and Akopova, 2003).

Measuring anisotropy

Static anisotropy was measured with a low aperture lens (10×, $NA = 0.22$) using wide-field microscopy. The polarization direction of exciting light was kept constant to minimize distortion of polarized light by microscope optics. To measure orthogonal polarizations, fiber axis was rotated by 90°. Otherwise, the measurements were made as described before (Borejdo et al., 2002a,b).

Dynamic anisotropy were measured with a high aperture lens (C-Apo, 40×, $NA = 1.2$) using confocal microscopy. Measurement of absolute anisotropies in the confocal microscope is complicated by unequal sensitivities of the photodetectors and by the mixing of orthogonally polarized emitted light by the high numerical aperture (NA) objective. To estimate sensitivities, the analyzers in front of both photomultipliers were placed in the same orientation. In this case, both channels must produce identical images. The voltages controlling brightness and contrast of both PMs were adjusted until control images were identical. In our microscope, the ratio of voltages controlling detectors of channels 1 and 2 had to be set at 0.92. The effect of high NA on anisotropy was corrected according to Axelrod (1979). He pointed out that the observed polarized fluorescence intensities are weighted averages of the three components of the polarized fluorescence intensities emitted at the sample, F_x, F_y, and F_z. Expressions for F_x, F_y, and F_z were derived for fluorescence-labeled cross-bridges in the muscle fiber (Burghardt et al., 2001). There, many cross-bridges were in the observed volume and the probe angular distribution was independent of the azimuthal angle describing the probe distribution at the fiber symmetry axis. In the present application where ~1000 fluorophores are detected, probe distribution symmetry at the fiber axis is likewise appropriate. Other fixed parameters contributing to F_x, F_y, and F_z are the aperture angle σ, the angle between probe absorption and emission dipoles, ξ, and the extent of independent probe movement while the probe is bound, δ. The water immersion objective used in the time-resolved experiments had $NA = 1.2$ giving $\sigma = \sim 64°$. To estimate ξ and δ we measured excitation spectra of Rh-phalloidin-actin in 90% glycerol (Fig. 4 *A*). The limiting anisotropy, r_o, of Rh-phalloidin on F-actin at $\lambda_{ex} = 568$ nm and $\lambda_{em} > 580$ nm was 0.373, giving the angle $\xi = 12°$. The anisotropy of Rh-phalloidin bound to F-actin tumbling in buffer solution was $r \approx 0.248$ (Fig. 4 *A*). Comparing r_0 and r indicates the extent of probe movement in solution. The fluorescence lifetime of rhodamine probe is much shorter than the rotational relaxation

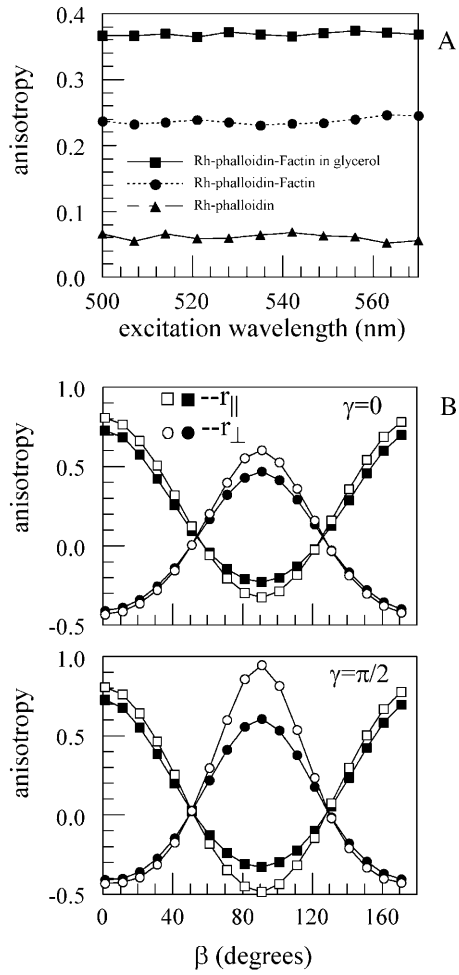

FIGURE 4 (*A*) Fluorescence anisotropy excitation spectra of Rh-phalloidin. 0.1 μM free Rh-phalloidin, ▲; 0.1 μM Rh-phalloidin bound to 5 μM F-actin, ●; and 0.1 Rh-phalloidin bound to 5 μM F-actin in the presence of 90% glycerol, ■. Measurements were made at room temperature except when glycerol was present (0°C). $\lambda_{em} > 580$ nm. (*B*) Comparing the expected $R_{\parallel}$ (*squares*) and $R_{\wedge}$ (*circles*) detected from $NA = 1.2$ (*solid symbol*) and $NA = 0.02$ (*open symbol*) microscope objectives. The $NA = 0.02$ curves represents the case when the objective numerical aperture has no detectable effect on observed anisotropy. The angles β and γ correspond to the polar and torsional position of the average probe dipole fixed frame relative to the laboratory fixed frame that has the z axis parallel to the fiber symmetry axis and the y axis parallel to the microscope optical axis. The average probe dipole fixed frame is so designated because the probe rotates independently within infinite square well potentials and the average frame is fixed to the midpoints of the wells. Assuming for this calculation that the emission dipole moment is parallel to the z axis of a probe fixed frame and the absorption dipole moment lies in the x,z plane, these dipoles are rotating independently and quickly on the timescale of the fluorescence lifetime in their polar and torsional degrees of freedom limited by the well potentials that are 30° wide. Curves plotted as a function of β for $\gamma = 0$ (*upper*) and $\pi/2$ (*lower*) are appropriate for the rhodamine probe with 12° between absorption and emission dipoles. The $\gamma = 0$ and $\gamma = \pi/2$ curves represent extreme cases. Comparison of solid and open symbols show that at $\beta \approx 45°$, high or low NA objectives produce the same anisotropy.

time of Rh-phalloidin-F-actin complex suggesting that the rotation of the complex cannot depolarize the rhodamine fluorescence and lower r from its limiting value. Rather, the local probe movement causes depolarization. The two degrees of freedom, corresponding to the polar and torsional movement of a reference frame fixed to the probe, describes the local probe movement. The anisotropy data is consistent with local polar and torsional probe movement within an infinitely deep square well potential $\delta \approx 30°$ wide. Using $\sigma = 64°$, $\xi = 12$, and $\delta = 30°$ and estimating the cross-bridge angle from wide-field measurements at ~45° (see below), Fig. 4 *B* indicates that the high NA of the objective introduces no significant error in the anisotropy estimate.

Let subscripts before and after the intensity indicate the direction of polarization of exiting and emitted light relative to the axis of the muscle fiber. Perpendicular anisotropy is recorded with the $\lambda/2$ plate in place. With muscle axis oriented horizontally on a stage of a microscope, channels 1 and 2 record ${}_{\perp}I_{\perp}$ and ${}_{\perp}I_{\parallel}$, respectively. Parallel anisotropy is recorded with the $\lambda/2$ absent. With muscle axis horizontal, channels 1 and 2 record ${}_{\parallel}I_{\perp}$ and ${}_{\parallel}I_{\parallel}$, respectively. The "on-screen-anisotropy" $R_{\perp}$ is defined as (ch1 − ch2)/(ch1 + 2 × ch2) × 256 + 128 and $R_{\parallel}$ as (ch2 − ch1)/(ch1 + 2 × ch2) × 256 + 128. Factors 256 and 128 make R visible on an 8-bit display. The absolute anisotropies are $r_{\perp} = (\text{ch1} - \text{ch2})/(\text{ch1} + 2 \times \text{ch2})$ and $r_{\parallel} = (\text{ch2} - \text{ch1})/(\text{ch1} + 2 \times \text{ch2})$.

RESULTS

Static anisotropy

Table 2 summarizes static anisotropy data. In Rh-phalloidin-labeled fibers, the anisotropy was large in rigor when the fiber axis was parallel to the direction of the polarization of exciting light and small when it was perpendicular. This suggests that the absorption/emission dipole of Rh-phalloidin is oriented largely parallel to the muscle axis and is in agreement with earlier data (Borovikov et al., 1996; Zhukarev et al., 1997). The excitation anisotropy spectrum of immobilized dye (Fig. 4, *top*) suggests that the angle between absorption and emission dipoles is 12°. Upon transition to relaxation, the parallel anisotropy decreased and perpendicular anisotropy increased, suggesting that the dipoles are now more perpendicular to muscle axis. Assuming the Gaussian distribution of dipoles at the muscle axis (Thomas and Cooke, 1980; Wilson and Mendelson, 1983), the angles of Rh-phalloidin dipoles with respect to the fiber axis were estimated by the method of Xiao et al. (1995) as 42° ± 20° in rigor and 47° ± 24° in relaxation. Table 2 suggests that the angle for Alexa-ATP-labeled actin was largely perpendicular to muscle axis. Changes associated with relaxation are small, reflecting the fact that the fluorescence lifetime of Alexa-ATP is short (~2 ns) and that it is not immobilized on the surface of actin (see below).

TABLE 2 Static anisotropies

	$R_{\parallel}$	$R_{\perp}$
Rigor (Rh-phalloidin)*	0.333 ± 0.018†	−0.026 ± 0.043
Relax (Rh-phalloidin)	0.272 ± 0.014	0.122 ± 0.026
Rigor (Alexa-ATP)‡	0.144 ± 0.014	0.119 ± 0.008
Relax (Alexa-ATP)	0.152 ± 0.017	0.091 ± 0.013

The anisotropies were measured in a wide-field microscope using 10× (*NA* = 0.22) objective. They are defined as: $R_{\perp} = ({}_{\perp}I_{\perp}/C_{\perp} - {}_{\perp}I_{\parallel})/({}_{\perp}I_{\perp}/C_{\perp} + 2{}_{\perp}I_{\parallel})$, and $R_{\parallel} = ({}_{\parallel}I_{\parallel}/C_{\parallel} - {}_{\parallel}I_{\perp})/({}_{\parallel}I_{\parallel}/C_{\parallel} + 2{}_{\parallel}I_{\perp})$, where the Cs are correction factors accounting for depolarization of light by microscope optics. The fiber, not the polarization of exciting light, was rotated by 90° to make $C_{\perp} = C_{\parallel}$. Using Chroma rhodamine and Cy5 dichroic mirrors, $C = 1.1$ and 0.98, respectively. The anisotropy R is related to the polarization of fluorescence P by $R = 2P/(3–P)$.

*Rh-phalloidin on actin.

†Mean ± SE, $n = 5$.

‡Alexa647-ATP on actin. Excitation at 633 nm.

Changes of anisotropy of actin labeled with Rh-phalloidin

The rationale was to observe a small population of actin monomers, to synchronize motion by rapid application of ATP and to follow the orientation changes associated with binding and hydrolysis by myosin of a single molecule of ATP. Muscle actin was labeled with Rh-phalloidin, fiber was placed horizontally on a stage of a confocal microscope and observed through a long-pass filter ($\lambda > 590$ nm). The objective focused visible laser light onto the I-band (*white spot* in Fig. 2 *A*). The laser beam was focused slightly off-center of the fluorescent band to avoid taking measurements from the Z-line and from the tips of the actin filaments. The laser beam was not scanned, i.e., the same actin molecules were observed throughout the experiment. This has an important advantage over earlier experiments (Borejdo et al., 2002b) in that the same fluorophores are observed throughout the entire experiment and that only a short pulse of UV radiation is necessary to produce ATP. Unfortunately, it causes considerable photobleaching because the same fluorophores are under constant illumination. To decrease photobleaching the laser beam was attenuated 300–1000 times. 262,144 (512 × 512) measurements are taken every 25 μs for a total of 6.55 s. 570 or 130 data points are averaged to display anisotropy every 14.25 or 3.25 ms. The video card (Matrox Imaging Series, Matrox, Dorval, Québec, Canada) calculates the perpendicular or parallel on-screen-anisotropy in real-time.

The rotations were synchronized by the sudden photogeneration of ATP from caged precursor. Approximately 3 s after the beginning of the experiment, the shutter admitting the UV light is opened for exactly 10 ms. It produces 2 mM ATP in the illuminated volume. The diffusion coefficient of ATP is $3.7 \times 10^{-6}/\text{cm}^2$ per second (Hubley et al., 1996), so ATP diffuses away from the experimental volume in ~300 μs. Although the actual diffusion coefficient in filament lattice of muscle fiber may be smaller, this order-of-magnitude calculation shows that soon after the application of a pulse there is practically no free nucleotide in the experimental volume. The sole nucleotide remaining in the volume is the one bound to the cross-bridge. The anisotropy change after the pulse reflects actin rotation induced by a turnover of this molecule of ATP.

Fig. 5 *A* is a plot of the perpendicular anisotropy of fluorescence of actin labeled with Rh-phalloidin. The on-

screen-anisotropy $R_{\perp}(t) = [({}_{\perp}I_{\perp}(t) - {}_{\perp}I_{\parallel}(t))/({}_{\perp}I_{\perp}(t) + 2{}_{\perp}I_{\parallel}(t))] \times 256 + 128$) was calculated in real-time. 3.25 s after the beginning of experiment, a 10-ms pulse of UV light was applied to muscle (*arrow*). This pulse briefly converts the solution in which muscle is bathed from Ca-rigor to contracting. The rate of photobleaching just before applying the UV pulse was ~2.4% per second. Anisotropy decreased by 16% during the course of the experiment (without the application of the UV pulse). This photobleaching was subtracted from the raw data, which after conversion to $r_{\perp}$ gave the data of Fig. 5 *B*. The anisotropy changes consisted of a rapid increase followed by a slow relaxation to a new steady-state level.

To measure the rate of anisotropy change, the time resolution was increased. The results are shown in Fig. 6 *A*. In this plot 130 data points (rather than 570) were averaged to increase the time resolution to 3.25 ms. In 16 experiments the average half-time of rapid change was 81 ± 25 ms (mean ± SE). The average half-time of myosin head reorientation (reflecting cross-bridge dissociation from thin filaments) was 130 ± 20 ms (Borejdo and Akopova, 2003), not statistically different from actin rotation. The significance of these findings is explored in the Discussion. The rapid increase was followed by a slow relaxation to a new steady-state value. The average half-time of this process was 478 ± 36 ms (n = 16). The average half-time of cross-bridge reorientation (reflecting rebinding to thin filaments) was 660 ± 100 ms (Borejdo and Akopova, 2003), again not statistically different from actin rotation. Approximately 1.5 s after the pulse, the anisotropy assumed new steady-state value. This was always different from the initial rigor value. It is speculated (see Discussion) that this fact reflects different state of actin before and after creation of ATP. (The reason the rates are so slow is because these are single turnover experiments. This slows

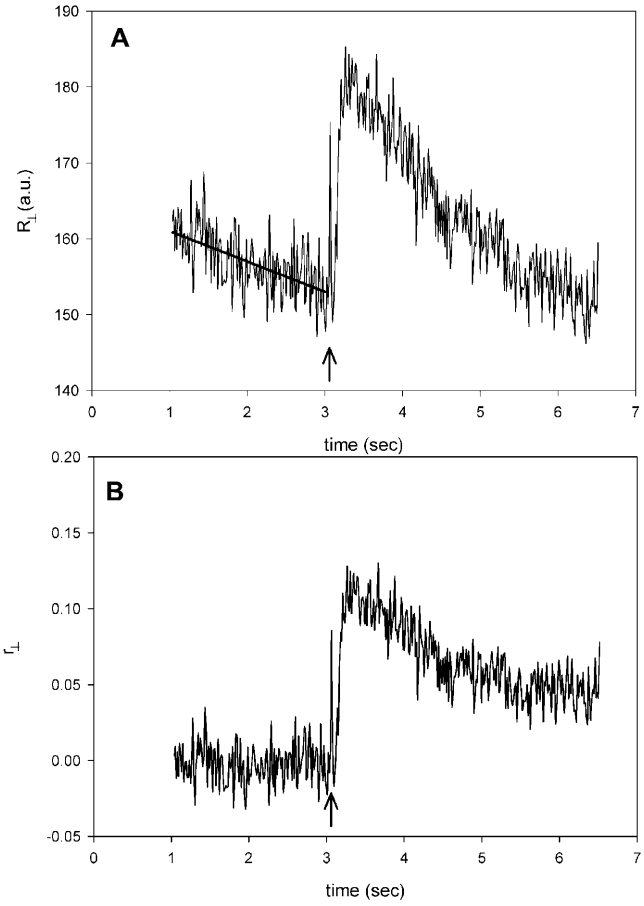

FIGURE 5 Perpendicular anisotropy of Rh-phalloidin bound to thin filaments of muscle fiber. (*A*) On-screen anisotropy $R_{\perp}(t) = [({}_{\perp}I_{\perp}(\text{ch1}) - {}_{\perp}I_{\parallel}(\text{ch2}))/({}_{\perp}I_{\perp}(\text{ch1}) + 2{}_{\perp}I_{\parallel}(\text{ch2}))] \times 256 + 128$. Solid line is a fit used to de-trend the data to account for photobleaching. (*B*) Data after correcting for photobleaching. The anisotropy $r_{\perp}(t) = [({}_{\perp}I_{\perp}(\text{ch1}) - {}_{\perp}I_{\parallel}(\text{ch2}))/({}_{\perp}I_{\perp}(\text{ch1}) + 2{}_{\perp}I_{\parallel}(\text{ch2}))]$ has been adjusted to 0 before photogeneration of ATP to correspond to static value of Table 2. The fiber in Ca^{2+}-rigor solution. Pulse of ATP is generated at arrows.

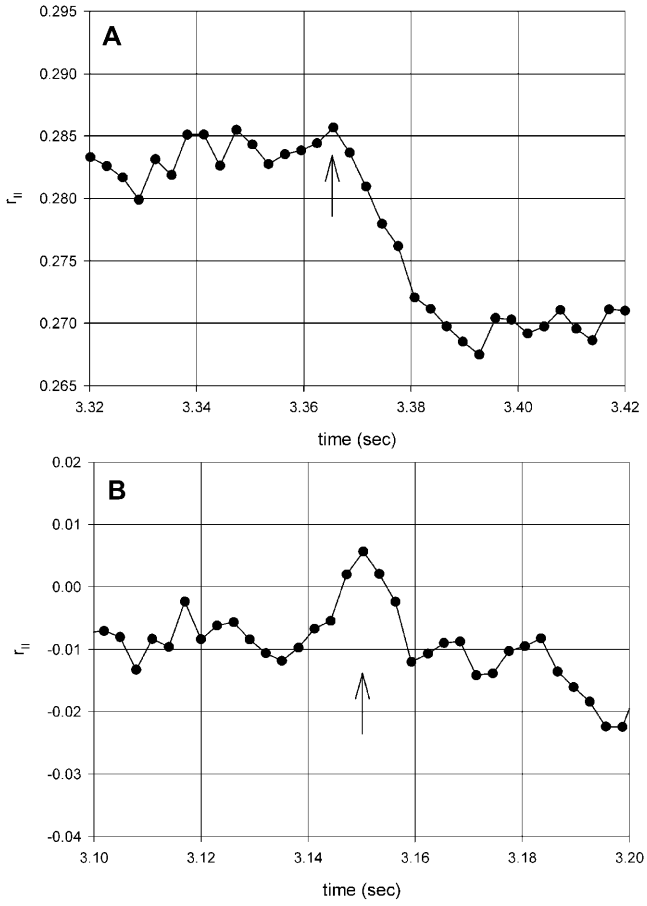

FIGURE 6 Parallel anisotropy of Rh-phalloidin bound to thin filaments of muscle fiber. (*A*) Anisotropy $r_{\parallel} = [({}_{\parallel}I_{\parallel}(\text{ch2}) - {}_{\parallel}I_{\perp}(\text{ch1}))/({}_{\parallel}I_{\parallel}(\text{ch2}) + 2{}_{\parallel}I_{\perp}(\text{ch1})]$ has been corrected for PM sensitivities and for photobleaching (the NA of the objective does not affect the measured anisotropy according to Fig. 4 *B*). 130 points are averaged to give time resolution of 3.25 ms. (*B*) Control anisotropy showing that there are no changes when analyzers in both channels are parallel, $r_C(t) = [({}_{\parallel}I_{\parallel}(\text{ch2}) - {}_{\parallel}I_{\parallel}(\text{ch1}))/({}_{\parallel}I_{\parallel}(\text{ch2}) + 2{}_{\parallel}I_{\parallel}(\text{ch1})]$. The fiber in Ca^{2+}-rigor solution. Pulse of ATP is generated at arrows.

down dissociation approximately 15 times and rebinding approximately three times; see Borejdo and Akopova, 2003.)

In our experiments the perpendicular and parallel anisotropies could not be measured simultaneously, because the microscope did not contain Pockel's cell to rotate the direction of the excitation polarization. However, parallel anisotropy could be measured after the perpendicular one by manually rotating the plane of polarization by half-wave plate. Fig. 6 shows one such experiment. Fig. 6 *B* shows an important control. Here the control anisotropy is defined as the difference between the intensities in channels 1 and 2 divided by their sum when analyzers in channels 1 and 2 have the same orientation, i.e., $r_C(t) = [({}_{\|}I_{\|}\ (\mathrm{ch2}) - {}_{\|}I_{\|}\ (\mathrm{ch1}))/({}_{\|}I_{\|}\ (\mathrm{ch2}) + 2{}_{\|}I_{\|}\ (\mathrm{ch1})$. Under those conditions the intensity recorded by both channels has the same polarization and therefore anisotropy change must be 0. The fact that it is so, is a convincing demonstration that the measurements are not artifacts due to heating of the experimental volume by the UV light (see Discussion).

Anisotropy of "ghost" fibers

To see whether myosin was necessary for the reorientation of actin, experiments were done on ''ghost'' fibers devoid of thick filaments. A fiber was first tested for rotation of actin. Myosin was then extracted from the same fiber by the application of Hasselbach-Schneider solution (0.47 M KCl, 5 mM $MgCl_2$, 10 mM PP_i, and 0.1 M PO_4 buffer, at pH 6.4) for 10 min at room temperature followed by extensive washing with Ca^{2+}-rigor solution. After myosin extraction, there was no change of anisotropy after photogeneration of ATP (not shown). The same results were obtained in three experiments on three different batches of fibers.

Anisotropy of actin labeled with fluorescent ATP

Fig. 7 *A* shows the appearance of a fiber labeled with Alexa-ATP. Only the I-bands are fluorescent. Fig. 7 *B* is the fluorescence anisotropy of Alexa-ATP incorporated into F-actin in solutions containing glycerol, in buffer, and free in buffer. Limiting anisotropy from the sample in glycerol, $r_o = 0.4$, is the theoretical maximum consistent with co-linear absorption and emission dipole moments. Rotational relaxation of F-actin is much slower than fluorescence lifetime of Alexa-ATP (~2 ns) such that the fluorescence anisotropy of Alexa-ATP in F-actin in buffer decreases from its limiting value only due to independent movement of the chromophore in its binding site. In a calculation analogous to that used for the rhodamine probe in Rh-phalloidin, the anisotropy data is consistent with local polar and torsional probe movement within infinitely deep square well potentials with width $\delta = 45°$. The residual anisotropy for free Alexa-ATP implies the isotropic tumbling of the probe is not rapid enough to fully depolarize the emitted light during fluorescence lifetime of the probe. Comparison of limiting and residual anisotropies suggests that rotational relaxation time of free Alexa-ATP is approximately equal to its fluorescence lifetime.

Fig. 8 *A* shows transient anisotropy of Alexa-ATP incorporated into thin filaments. Because anisotropies of free Alexa-ATP and Alexa-ATP incorporated into F-actin are equal (Fig. 7 *B*), these changes do not arise from the change in nanosecond-timescale anisotropy, but must result from actin rotation. After the flash (*arrow*), the anisotropy

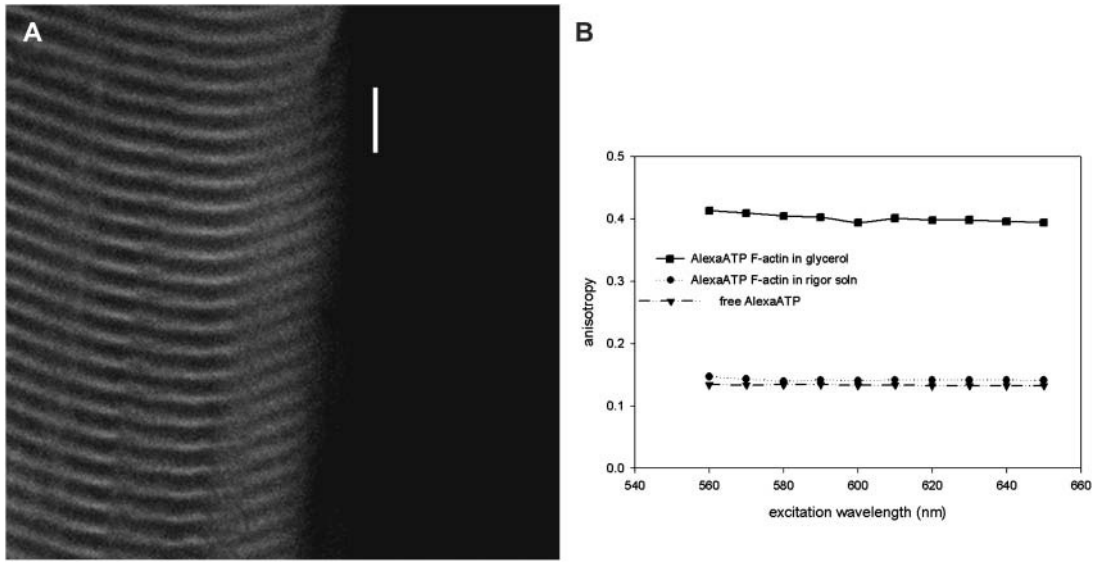

FIGURE 7 (*A*) Fiber labeled with Alexa-ATP. The I-bands are fluorescent. Fiber viewed through Cy5 filter (long-pass $\lambda > 675$ nm). Bar = 10 μm. (*B*) Excitation anisotropy of Alexa-ATP. 1 μM of free Alexa-ATP in Ca-rigor, ▼; 2 μM F-actin + 1 μM Alexa-ATP in Ca-rigor, ●; and 2 μM F-actin + 1 μM Alexa-ATP in 90% glycerol, ■. Emission wavelength = 670 nm, 0°C.

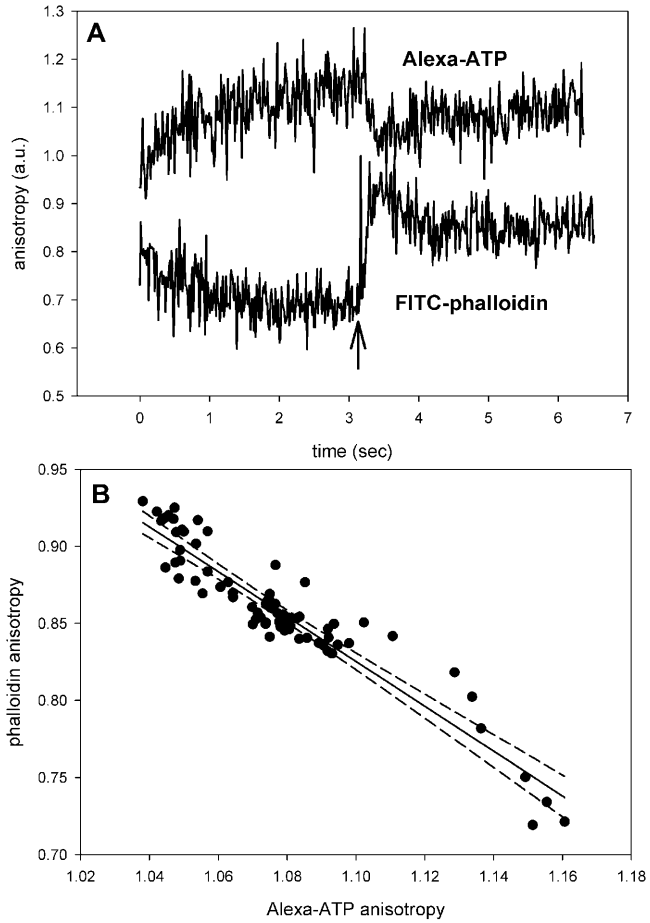

FIGURE 8 The rotation of actin labeled at the nucleotide site by fluorescent nucleotide and at the phalloidin site by phalloidin. (*A*, *top*) Actin labeled with Alexa-ATP; (*A*, *bottom*) actin labeled with FITC-phalloidin. Arrow indicates the flash of UV light. (*B*) The correlation between the top and bottom curves between $t = 3$ and 4 s. Curves were smoothed by a running average and linearly correlated ($r^2 = 0.886$). 99% confidence limits are indicated by dashed lines.

changes rapidly before relaxing to a new value. The response was the same when actin was labeled with Cy5-ATP (data not shown).

The kinetics of the orientational change of actin labeled with Alexa-ATP was identical to the kinetics of actin labeled with phalloidin. The bottom and top curves in Fig. 8 *A* is the experiment in which actin was labeled with phalloidin and Alexa-ATP, respectively (unfortunately, the experiment could not be done on the same fiber because phalloidin inhibits changes of anisotropy of nucleotide). For this reason, the curves had to be scaled to fit on the same graph and anisotropy is in arbitrary units. Inspection reveals that the two curves are similar. To quantify this similarity, we compared the smoothed anisotropy change of Alexa-ATP and phalloidin bound to actin between 3 and 4 s. Fig. 8 *B* is a plot of two traces plotted against each other. Each point represents a pair of anisotropies from Alexa-ATP- and phalloidin-labeled fibers of Fig. 8 *A* taken at the same time. It suggests that the anisotropies are closely correlated; the dashed lines show 99% confidence limits. We conclude that the anisotropy change of Alexa-ATP bound to actin reflects the rotation of Alexa-ATP bound to actin monomers, and not the change of anisotropy due to the release of ADP from monomers during cross-bridge turnover. The significance of this finding is explored in the Discussion.

DISCUSSION

Ruling out the artifacts

The artifacts may arise because of 1), heating of muscle; 2), damage to muscle fiber induced by the UV light; and 3), motion of fiber. We argue that none of the above is responsible for the present observations.

1. Heating: The heating is caused by the absorption of UV light by caged ATP. Extinction coefficient of caged-ATP at 364 nm is 4400 M^{-1}/cm^{-1}, i.e., 3-μm-thick section of muscle perfused with 2 mM precursor absorbs 0.264% of the incident UV light. Because beam diameter is small, the heat associated with this absorption dissipates in $<\sim$70 ns (Denk et al., 1995). The UV laser delivers 0.9×10^{-11} J in 70 ns, i.e., temperature rise during the experiment is <2°C. The experimental support of this argument is the observation that the UV pulse did not cause change in the control anisotropy (Fig. 6 *B*). The only difference between the control and actual anisotropy measurements is the orientation of analyzer in channel 1. In control experiments both analyzers have the same orientation. In actual experiments the data is obtained from a neighboring sarcomere and the only difference is that the orientation of analyzer in channel 1 is orthogonal to channel 2. The sample is subjected to the identical dose of UV light. Yet control shows no change of anisotropy. There are three additional lines of evidence to suggest that anisotropy change does not reflect temperature rise in the experimental volume. Firstly, caged EDTA (DMNP-EDTA), which has the same UV absorption as caged ATP, caused no change of anisotropy whatsoever (data not shown). Secondly, there is no anisotropy change in denatured fibers (left for 24 h at room temperature, data not shown). Finally, fibers devoid of myosin did not give any anisotropy change upon stimulation by caged ATP.
2. Damage: Muscle damage caused by the exposure to the UV light can be eliminated as a possible source because there was no anisotropy change whatever in fibers which did not contain caged ATP but were exposed to the UV pulse (data not shown).
3. Motion: The mean concentration of ATP in the experimental chamber photogenerated in each experiment is $\sim 6 \times 10^{-8}$ mM. This is too small to induce global contraction. There was no evidence of a local contraction either, inasmuch as when the image of a fiber taken before the

contraction is subtracted from the image taken after the contraction, the result is 0 (black) everywhere except in the area where photobleaching occurred (data not shown).

Actin labeled with Rh-phalloidin

Results summarized in Table 2 suggest that the emission dipole of Rh-phalloidin undergoes ~5° change in angle upon photogeneration of ATP. The observed changes are due to rotation of at least 50% of all actin monomers, rather than to a small fraction of actins rotating a lot, averaged with a much larger number that do not move at all. This is because in our experiments muscle is initially in rigor, where approximately one-half of actins have a cross-bridge associated with it. We think that the whole thin filament begins to undulate during contraction, as originally proposed by Ishiwata and Oosawa (1974).

The kinetics of change revealed that actin rotated in two phases. The experiments using ghost fibers show that myosin is necessary for all phases to occur. The first phase was a fast reorientation. The half-time of this process was ~80 ms, not significantly different than the rate of cross-bridge dissociation (Borejdo and Akopova, 2003). Coincidence of changes in actin and dissociation are consistent with earlier observation that saturation transfer electron paramagnetic resonance spectra of spin labels on Cys-374 of actin changed upon dissociation of S1 (Thomas et al., 1979) and with observation that binding of S1 to actin labeled with spin labeled analogs of ATP resulted in some change in actin conformation (Naber and Cooke, 1994). Preliminary data obtained from the same muscle fiber in which myosin and actin were labeled (with fluorescent regulatory light chain and phalloidin, respectively), suggested coincidence of cross-bridge dissociation and orientation changes of actin. We conclude that actin orientation changes are caused by cross-bridge dissociation, and do not indicate active rotation of actin. However, we cannot rule out the possibility that the changes in actin occur before changes in myosin. Rapid changes in actin could be due to the activation process. This may be related to earlier findings (Huxley et al., 1994; Bordas et al., 1999) that there was a small decrease in the spacing of the axial repeat of actin during contraction against the negligible load.

The second phase of the anisotropy change was slow relaxation to a steady-state value. The half-time of this process was ~480 ms, again not significantly different from cross-bridge binding to thin filaments in single-turnover experiments (Borejdo and Akopova, 2003). We think that this process reflects binding of cross-bridges.

The second phase of anisotropy change ended with a resumption of a new steady-state value, typically 1.5–2 s after the pulse. This value was always different from the initial rigor value. A possible explanation of this result is that thin filaments are in different state before and after the exposure to a pulse of ATP. Before the exposure the thin filaments are under stress because muscle develops full rigor tension when it is transferred from relaxing (glycerinating) solution to rigor solution. After the exposure, however, the filaments are unstressed because muscle does not develop rigor tension during single-turnover experiment.

Active role of actin in contraction

This requires that actin hydrolyzes ATP, i.e., that during muscle contraction strongly bound ADP is exchanged with ATP in solution. The present results suggest that this does not occur, i.e., that the nucleotide remains actin-bound during muscle contraction. Firstly, the anisotropies of free Alexa-ATP and Alexa-ADP bound to thin filaments are the same (Fig. 7 *B*), i.e., 10% changes in anisotropy of Alexa-ATP incorporated into thin filaments, such as recorded in Fig. 8 *A*, must result from actin rotation and not from the release of the probe into solution. Secondly, the time-course of decline of anisotropy of ADP approximates the change of anisotropy of phalloidin, which stays attached to actin at all times. This suggests that ADP also stays attached to actin. It is unlikely that ADP comes off actin so late that it would not be detected in our experiment. ATPase of muscle at 20°C is ~5 s^{-1} (Houadjeto et al., 1992), i.e., ADP dissociates with half-time of ~140 ms, easily within the timescale of our experiment. It is also unlikely that the fraction of actin-bound nucleotide undergoing dissociation is too small to be detected. The molar ratio of actin to myosin in skeletal muscle is ~5:2 (Bagshaw, 1982), i.e., if the hydrolysis of ATP by actin were powering muscle contraction, 40% of actin monomers would have to release ADP. The confidence that the changes of the anisotropy of phalloidin- and fluorescent nucleotide-ATP were the same was high (Fig. 8 *B*).

Supported by National Institutes of Health grants R21CA9732 and R01AR048622 and by the Texas Higher Education Coordinating Board grant 000130-0008-2001 (to J.B.), and National Institutes of Health grant R01AR39288 and the Mayo Foundation (to T.P.B.).

REFERENCES

Allen, T. S.-C., N. Ling, M. Irving, and Y. E. Goldman. 1996. Orientation changes in myosin regulatory light chains following photorelease of ATP in skinned muscle fibers. *Biophys. J.* 70:1847–1862.

Ao, X., and S. S. Lehrer. 1995. Phalloidin unzips nebulin from thin filaments in skeletal myofibrils. *J. Cell Sci.* 108:3397–3403.

Axelrod, D. 1979. Carbocyanine dye orientation in red cell membrane studied by microscopic fluorescence polarization. *Biophys. J.* 26:557–573.

Bagshaw, C. R. 1982. Muscle Contraction. Chapman & Hall, London, UK.

Barany, M., J. T. Barron, L. Gu, and K. Barany. 2001. Exchange of the actin-bound nucleotide in intact arterial smooth muscle. *J. Biol. Chem.* 276:48398–48403.

Bordas, J., A. Svensson, M. Rothery, J. Lowy, G. P. Diakun, and P. Boesecke. 1999. Extensibility and symmetry of actin filaments in contracting muscles. *Biophys. J.* 77:3197–3207.

Borejdo, J., and I. Akopova. 2003. Orientational changes of cross-bridges during single turnover of ATP. *Biophys. J.* 84:2450–2459.

Borejdo, J., O. Assulin, T. Ando, and S. Putnam. 1982. Cross-bridge orientation in skeletal muscle measured by linear dichroism of an extrinsic chromophore. *J. Mol. Biol.* 158:391–414.

Borejdo, J., D. S. Ushakov, and I. Akopova. 2002a. The essential light chains 1 and 3 rotate differently during muscle contraction. *Biophys. J.* 82:362A.

Borejdo, J., D. S. Ushakov, and I. Akopova. 2002b. The regulatory and essential light chains of myosin rotate equally during contraction of skeletal muscle. *Biophys. J.* 82:3150–3159.

Borovikov, Y. S., and N. A. Chernogriadskaia. 1979. Studies on conformational changes in F-actin of glycerinated muscle fibers during relaxation by means of polarized ultraviolet fluorescence microscopy. *Microsc. Acta.* 81:383–392.

Borovikov, Y. S., D. I. Levitskii, V. P. Kirillina, and B. F. Poglazov. 1982. Effect of Ca^{2+} binding to 5,5′-dithiobis(2-nitrobenzoic acid) light chains on conformational changes of F-actin caused by myosin subfragment-1. *Eur. J. Biochem.* 125:343–347.

Borovikov, Y. S., K. Y. Horiuchi, S. V. Avrova, and S. Chacko. 1996. Modulation of actin conformation and inhibition of actin filament velocity by calponin. *Biochemistry.* 35:13849–13857.

Bukatina, A. E., F. Fuchs, and S. C. Watkins. 1996. A study on the mechanism of phalloidin-induced tension changes in skinned rabbit psoas muscle fibres. *J. Muscle Res. Cell Motil.* 17:365–371.

Burghardt, T. P., A. R. Cruz-Walker, S. Park, and K. Ajtai. 2001. Conformation of myosin interdomain interactions during contraction: deductions from muscle fibers using polarized fluorescence. *Biochemistry.* 40:4821–4833.

Denk, W., D. W. Piston, and W. W. Webb. 1995. Two-photon molecular excitation in laser-scanning microscopy. *In* Handbook of Biological Confocal Microscopy. J. Pawley, editor. Plenum Press, New York and London.

Dos Remedios, C. G., R. G. Millikan, and M. F. Morales. 1972. Polarization of tryptophan fluorescence from single striated muscle fibers. A molecular probe of contractile state. *J. Gen. Physiol.* 59:103–120.

Fujita, H., and S. Ishiwata. 1998. Spontaneous oscillatory contraction without regulatory proteins in actin filament-reconstituted fibers. *Biophys. J.* 75:1439–1445.

Galkin, V. E., M. S. VanLoock, A. Orlova, and E. H. Egelman. 2002. A new internal mode in F-actin helps explain the remarkable evolutionary conservation of actin's sequence and structure. *Curr. Biol.* 12:570–575.

Goldman, Y. E., M. G. Hibberd, and D. R. Trentham. 1984. Initiation of active contraction by photogeneration of adenosine-5′-triphosphate in rabbit psoas muscle fibres. *J. Physiol.* (*Lond.*). 354:605–624.

Hopkins, S. C., C. Sabido-David, J. E. Corrie, M. Irving, and Y. E. Goldman. 1998. Fluorescence polarization transients from rhodamine isomers on the myosin regulatory light chain in skeletal muscle fibers. *Biophys. J.* 74:3093–3110.

Houadjeto, M., F. Travers, and T. Barman. 1992. Ca^{2+}-activated myofibrillar ATPase: transient kinetics and the titration of its active sites. *Biochemistry.* 31:1564–1569.

Hubley, M. J., B. R. Locke, and T. S. Moerland. 1996. The effects of temperature, pH, and magnesium on the diffusion coefficient of ATP in solutions of physiological ionic strength. *Biochim. Biophys. Acta.* 1291: 115–121.

Huxley, A. F., and R. M. Simmons. 1971. Proposed mechanism of force generation in striated muscle. *Nature.* 233:533–538.

Huxley, H. E., A. Stewart, H. Sosa, and T. Irving. 1994. X-ray diffraction measurements of the extensibility of actin and myosin filaments in contracting muscle. *Biophys. J.* 67:2411–2421.

Ishiwata, S., and F. Oosawa. 1974. A regulatory mechanism of muscle contraction based on the flexibility change of the thin filaments. *J. Mechanochem. Cell Motil.* 3:9–17.

Naber, N., and R. Cooke. 1994. Mobility and orientation of spin probes attached to nucleotides incorporated into actin. *Biochemistry.* 33:3855–3861.

Nihei, T., R. A. Mendelson, and J. Botts. 1974. Use of fluorescence polarization to observe changes in attitude of S1 moieties in muscle fibers. *Biophys. J.* 14:236–242.

Nishikawa, S., K. Homma, Y. Komori, M. Iwaki, T. Wazawa, A. Hikikoshi Iwane, J. Saito, R. Ikebe, E. Katayama, T. Yanagida, and M. Ikebe. 2002. Class VI myosin moves processively along actin filaments backward with large steps. *Biochem. Biophys. Res. Commun.* 290: 311–317.

Oosawa, F. 1977. Actin-actin bond strength and the conformational change of F-actin. *Biorheology.* 14:11–19.

Oosawa, F., Y. Maeda, S. Fujime, S. Ishiwata, T. Yanagida, and M. Taniguchi. 1977. Dynamic characteristics of F-actin and thin filaments in vivo and in vitro. *J. Mechanochem. Cell Motil.* 4:63–78.

Ostap, E. M., and D. D. Thomas. 1991. Rotational dynamics of spin-labeled F-actin during activation of myosin S1 ATPase using caged ATP. *Biophys. J.* 59:1235–1241.

Page, R., U. Lindberg, and C. E. Schutt. 1998. Domain motions in actin. *J. Mol. Biol.* 280:463–474.

Prochniewicz-Nakayama, E., T. Yanagida, and F. Oosawa. 1983. Studies on conformation of F-actin in muscle fibers in the relaxed state, rigor, and during contraction using fluorescent phalloidin. *J. Cell Biol.* 97:1663–1667.

Sabido-David, C., B. Brandmeier, J. S. Craik, J. E. Corrie, D. R. Trentham, and M. Irving. 1998. Steady-state fluorescence polarization studies of the orientation of myosin regulatory light chains in single skeletal muscle fibers using pure isomers of iodoacetamidotetramethylrhodamine. *Biophys. J.* 74:3083–3092.

Spudich, J., and S. Watt. 1971. Regulation of rabbit muscle contraction. *J. Biol. Chem.* 246:4866–4871.

Strzelecka-Golaszewska, H., M. Jakubiak, and W. Drabikowski. 1975. Changes in the state of actin during superprecipitation of actomyosin. *Eur. J. Biochem.* 55:221–230.

Szczesna, D., and S. S. Lehrer. 1993. The binding of fluorescent phallotoxins to actin in myofibrils. *J. Muscle Res. Cell Motil.* 14:594–597.

Tanaka, H., K. Homma, A. H. Iwane, E. Katayama, R. Ikebe, J. Saito, T. Yanagida, and M. Ikebe. 2002. The motor domain determines the large step of myosin-V. *Nature.* 415:192–195.

Thomas, D. D., and R. Cooke. 1980. Orientation of spin-labeled myosin heads in glycerinated muscle fibers. *Biophys. J.* 32:891–905.

Thomas, D. D., J. C. Seidel, and J. Gergely. 1979. Rotational dynamics of spin-labeled F-actin in the sub-millisecond time range. *J. Mol. Biol.* 132:257–273.

Wilson, M. G. A., and R. A. Mendelson. 1983. A comparison of order and orientation of cross-bridges in rigor and relaxed muscle fibers using fluorescence polarization. *J. Musc. Res. Cell Mot.* 4:671–693.

Xiao, M., O. A. Andreev, and J. Borejdo. 1995. Rigor cross-bridges bind to two actin monomers in thin filaments of rabbit psoas muscle. *J. Mol. Biol.* 248:294–307.

Zhukarev, V., J. M. Sanger, J. W. Sanger, Y. E. Goldman, and H. Shuman. 1997. Distribution and orientation of rhodamine-phalloidin bound to thin filaments in skeletal and cardiac myofibrils. *Cell Motil. Cytoskeleton.* 37:363–377.